Utah State University
DigitalCommons@USU

CEE Faculty Publications | Civil and Environmental Engineering

1-1-2003

A Sediment Transport Model for Incision of Gullies on Steep Topography

E. Istanbulluoglu

D. G. Tarboton

Robert T. Pack
Utah State University

C. H. Luce

Recommended Citation
Istanbulluoglu, E., Tarboton, D.G., Pack, R.T., Luce, C. 2003. A sediment transport model for incision of gullies on steep topography. Water Resources Research, v.39, n.4, p.1103.

This Article is brought to you for free and open access by the Civil and Environmental Engineering at DigitalCommons@USU. It has been accepted for inclusion in CEE Faculty Publications by an authorized administrator of DigitalCommons@USU. For more information, please contact becky.thoms@usu.edu.

UtahStateUniversity
MERRILL-CAZIER LIBRARY

A sediment transport model for incision of gullies on steep topography

Erkan Istanbulluoglu,[1] David G. Tarboton, and Robert T. Pack
Department of Civil and Environmental Engineering, Utah State University, Logan, Utah, USA

Charles Luce
U.S. Forest Service, Rocky Mountain Research Station, Boise, Idaho, USA

Received 21 May 2002; revised 25 November 2002; accepted 26 February 2003; published 25 April 2003.

[1] We have conducted surveys of gullies that developed in a small, steep watershed in the Idaho Batholith after a severe wildfire followed by intense precipitation. We measured gully length and cross sections to estimate the volumes of sediment loss due to gully formation. These volume estimates are assumed to provide an estimate of sediment transport capacity at each survey cross section from the single gully-forming thunderstorm. Sediment transport models commonly relate transport capacity to overland flow shear stress, which is related to runoff rate, slope, and drainage area. We have estimated the runoff rate and duration associated with the gully-forming event and used the sediment volume measurements to calibrate a general physically based sediment transport equation in this steep, high shear stress environment. We find that a shear stress exponent of 3, corresponding to drainage area and slope exponents of $M = 2.1$ and $N = 2.25$, match our data. This shear stress exponent of 3 is approximately 2 times higher than those for bed load transport in alluvial rivers but is in the range of shear stress exponents derived from flume experiments on steep slopes and with total load equations. The concavity index of the gully profiles obtained theoretically from the area and slope exponents of the sediment transport equation, $\theta_c = (M - 1)/N$, agrees well with the observed profile concavity of the gullies. Our results, although preliminary because of the uncertainty associated with the sediment volume estimates, suggest that for steep hillslopes such as those in our study area, a greater nonlinearity in the sediment transport function exists than that assumed in some existing hillslope erosion models which calculate sediment transport capacity using the bed load equations developed for rivers. *INDEX TERMS:* 1815 Hydrology: Erosion and sedimentation; 1824 Hydrology: Geomorphology (1625); 1821 Hydrology: Floods; 1625 Global Change: Geomorphology and weathering (1824, 1886); *KEYWORDS:* gully erosion, sediment transport, landscape evolution

Citation: Istanbulluoglu, E., D. G. Tarboton, R. T. Pack, and C. Luce, A sediment transport model for incision of gullies on steep topography, *Water Resour. Res.*, *39*(4), 1103, doi:10.1029/2002WR001467, 2003.

1. Introduction

[2] Gullies are unstable, eroding channels formed at or close to valley heads, sides, or floors [*Schumm et al.*, 1984]. They usually differ from stable river channels in having steep sides, low width to depth ratios, and a head cut at the upslope end [*Knighton*, 1998]. The main causes of gully erosion are natural and anthropogenic effects that increase runoff production on hillslopes and/or reduce the erosion resistance of the soil surface. Some of these causes are the clearing of natural forests [*Prosser and Slade*, 1994; *Prosser and Soufi*, 1998], agricultural treatments and grazing [*Burkard and Kostaschuk*, 1995; *Vandekerckhove et al.*, 1998; *Vandekerckhove et al.*, 2000], climate change [*Coulthard et al.*, 2000], and road construction [*Montgomery*, 1994; *Wemple et al.*, 1996; *Croke and Mockler*, 2001]. Recent field observations of postfire erosion events in steep mountain drainages in the western United States also show that large pulses of sediment could be produced due to gully erosion [*Meyer et al.*, 2001; *Meyer and Wells*, 1997; *Cannon et al.*, 2001].

[3] There are two main stages of gully development: the incision stage, and the stability or infilling stage [*Sidorchuk*, 1999]. The initiation stage of gully erosion is often the most critical stage from a land management perspective, because once the gullies have initiated and developed it is difficult to control gully erosion [*Prosser and Soufi*, 1998; *Woodward*, 1999].

[4] In this paper we study the mechanistic behavior of sediment transport on steep mountains using gully erosion observations in a highly erodible steep forested basin in Idaho. These gullies were developed in a single rainstorm after a severe wildfire. We first theoretically adapt a general dimensionless sediment transport capacity equation to incis-

[1]Now at Department of Civil and Environmental Engineering, Massachusetts Institute of Technology, Cambridge, Massachusetts, USA.

Copyright 2003 by the American Geophysical Union.
0043-1397/03/2002WR001467$09.00

ing gullies by relating flow shear stress and width to contributing area and slope assuming steady state runoff generation and turbulent uniform flow conditions. The dimensionless sediment transport capacity relationship we used has two empirical parameters that need to be calibrated against data. We then present our field data comprising sediment volumes estimated from gully cross sections. Following this we calibrate the empirical parameters of the sediment transport equation to this field data and compare the results with the parameter ranges published in the literature.

1.1. Sediment Transport Review: Functional Form and Implications

[5] Sediment transport rate is often described as a power function of discharge and slope, or of shear stress [*Kirkby*, 1971; *Julien and Simons*, 1985; *Nearing et al.*, 1997]:

$$Q_s = k_1 Q^M S^N \tag{1}$$

$$Q_s = k_2(\tau - \tau_c)^p, \tag{2}$$

where Q_s is the rate of sediment transport in a channel, Q is water discharge, S is slope, τ is the average bottom shear stress, $\tau = \rho_w gRS$, where R is the hydraulic radius, ρ_w is water density, and g is gravitational acceleration. The τ_c is critical shear stress for incipient motion, k_1 is a rate constant, and k_2 is a transport coefficient. M, N, and p are model parameters. These functional forms are interchangeable when shear stress is written as a function of discharge and slope, $\tau \propto (Q, S)$ [*Willgoose et al.*, 1991a; *Tucker and Bras*, 1998].

[6] Many equations that describe sediment transport as a function of shear stress such as those of *Meyer-Peter and Muller* [1948] and Einstein-Brown and empirical total load sediment transport equations, for example, the Engelund and Hansen equation and the Bishop, Simons, and Richardson's methods, can be written in the form of equation (2) [*Garde and Raju*, 1985; *Chien and Wan*, 1999]. This equation is essentially based on the relationship between dimensionless sediment transport rate q_{s*} and dimensionless shear stress τ_*. Dimensionless sediment transport rate is commonly expressed as a nonlinear function of dimensionless shear stress in the form

$$q_{s*} = \beta \tau_*^p \tag{3}$$

where

$$q_{s*} = \frac{q_s}{\sqrt{g(s-1)d^3}} \tag{4a}$$

$$\tau_* = \frac{\tau/(\rho_w g)}{(s-1)d} \tag{4b}$$

$$\beta = \begin{cases} \kappa\left(1 - \dfrac{\tau_{*c}}{\tau_*}\right)^{p_\beta} & \tau_* > \tau_{*c} \\ 0 \text{ otherwise} \end{cases}. \tag{4c}$$

In these equations, q_s is the unit sediment discharge that could be either bed or total load; β is a dimensionless transport rate; s is the ratio of sediment to water density (ρ_s/ρ_w); d is dominant grain size, often taken as the median, d_{50}; τ_{*c} is dimensionless critical shear stress; the calibration parameters are κ, p, and p_β, and usually $p = p_\beta$. Dimensionless critical shear stress τ_{*c} is related to critical shear stress τ_c through equation (4b), similar to the nondimensionalization of shear stress. *Yalin* [1977] showed that κ is 17 at high values of τ_* for bed load transport. Many κ values were reported in the range of 4–40 in different equations [*Simons and Senturk*, 1977; *Yalin*, 1977]. The shear stress exponent p is consistently 1.5 for bed load equations developed for gentle slopes, while in total load equations it varies from relatively low values of $p \cong 1.5$ up to $p = 3$ depending on the mode of transport. Lower shear stress exponents correspond to predominantly bed load transport, and the higher values correspond to suspended sediment transport in the total load. Equation (3) does not fully describe the suspended load transport physics, and higher shear stress exponents for total load account for the additional sediment discharge due to suspended sediment in the same functional form used for bed load [*Garde and Raju*, 1985]. Nevertheless, total load equations in the form of equation (3) are easy to use and provide reasonable sediment transport capacity estimates [*Simons and Senturk*, 1977].

[7] Equation (1) has mathematical and computational advantages and is often used in landscape evolution models [*Smith and Bretherton*, 1972; *Tarboton et al.*, 1992; *Hancock and Willgoose*, 2001]. The discharge and slope exponents M and N in (1) are in the range of 1–2.5 [*Julien and Simons*, 1985; *Everaert*, 1991; *Rickenmann*, 1992; *Nearing et al.*, 1997]. The exponents M and N have significant impacts on hillslope evolution, drainage density, and landscape morphology [*Band*, 1990; *Arrowsmith et al.*, 1996; *Tucker and Bras*, 1998]. They influence landscape response timescales, duration and timing of erosional response, the sensitivity of mountain range relief to tectonic uplift, and the relief-uplift relationship [*Whipple and Tucker*, 1999; *Niemann et al.*, 2001; *Tucker and Whipple*, 2002].

[8] One of the long-term implications of a sediment transport relationship is the observed power law scaling of slope with contributing area, $S \propto A^{-\theta_c}$, where θ_c is the concavity index often in the range of 0.37–0.83 with a mean of 0.6 [*Tarboton et al.*, 1991]. For the case of dynamic equilibrium when the tectonic uplift is balanced by transport limited erosion, the power law relationship between local slope and upslope area is theoretically [*Willgoose et al.*, 1991b; *Tarboton et al.*, 1992]

$$S = \left(\frac{U}{k_1}\right)^{1/n} A^{-\theta_c}, \quad \theta_c = \frac{M-1}{N}, \tag{5}$$

where U is tectonic uplift or an average degradation rate and A is drainage area used as a proxy for discharge in the sediment transport equation (1). Some observations suggest that there may not be a great difference between the concavity of steady state and nonsteady state mountain basins. The Appalachians are believed to be in a state of decline, and yet Appalachian river basins reveal concavity indices consistent with the range often observed in steady

state topographies [*Willgoose*, 1994; *Tucker and Whipple*, 2002]. Discharge and slope exponents are the fundamental parameters of erosion and sediment transport and are related to the scale properties of landscape and river evolution used in landscape evolution research. Thus they are deserving of study via both fieldwork and modeling [*Rodriguez-Iturbe and Rinaldo*, 1997; *Tucker and Whipple*, 2002].

1.2. Sediment Transport on Steep Slopes

[9] Steep flume experiments suggest that bed load sediment transport can be described using equation (1) both for gentle and steep slopes when information about grain size and density is included in the equation [*Rickenmann*, 1991, 1992; *Mizuyama*, 1977; *Mizuyama and Shimohigashi*, 1985; *Smart and Jaeggi*, 1983]. A bed load transport equation was developed by *Smart and Jaeggi* [1983] based on their steep flume experiments using clear water and slope range 3–20% and the data of Meyer–Peter and Muller.

$$q_s = \frac{4}{(s-1)}\left(\frac{d_{90}}{d_{30}}\right)^{0.6}\left(1-\frac{\tau_{*c}}{\tau_*}\right)q_r S^{1.6}, \tag{6}$$

where q_r is the reduced unit discharge (corrected for sidewall influence) and d_{90} and d_{30} are the grain sizes at which 90% and 30% by weight of the sediment is finer. *Smart* [1984] suggested that for coarse alluvial sediments (mean grain size greater than 0.4 mm), observed sediment transport can be regarded as total load or the sediment transport capacity.

[10] *Rickenmann* [1991, 1992] conducted steep flume experiments using clay suspension as transporting fluid and analyzed his data with Smart and Jaeggi's data. He reported the following equation for both clear water and hyperconcentrated flows for slopes between 5% and 20%:

$$q_s = \frac{12.6}{(S-1)^{1.6}}\left(\frac{d_{90}}{d_{30}}\right)^{0.2}(q_r - q_{cr})S^2 \tag{7}$$

$$q_{cr} = 0.065(s-1)^{1.67}g^{0.5}d_{20}^{1.5}S^{-1.12}, \tag{8}$$

where q_{cr} is the critical discharge for the initiation of sediment motion. Equation (7) was originally proposed by *Bathurst et al.* [1987] and was slightly modified by Rickenmann to include the density factor $(s - 1)$. Rickenmann noted that as slopes increase, the exponents for $(s - 1)$ and S should increase as well. This observation was also supported by steep flume data of *Mizuyama and Shimohigashi* [1985], who predicted $q_s \propto S^2/(s-1)^2$ [*Rickenmann*, 1991].

[11] An inconsistency in equations (6) and (7) compared to other sediment transport studies on the same slope ranges is the discharge exponent. *Nearing et al.* [1997] combined experimental data for slopes between 0.5% and 30% and reported results in the form of (1) that consistently show a discharge exponent greater than 1.5. Equation (6) is linear with discharge, whereas equation (7) is linear for discharge in excess of a threshold. We do not know if median sediment size and density ratio factors considered in (4) and (6) account for the nonlinearity of sediment transport with respect to discharge that *Nearing et al.* [1997] found. A linear dependence of sediment transport on discharge has implications for erosion and landscape evolution dynamics. In the landscape form stability theory of *Smith and Bretherton* [1972], channels and concave hillslope profiles form when $M > 1$. In equation (5), $M = 1$ gives $\theta_c = 0$, which implies a constant slope or a planar topography. Such results can also be obtained from landscape evolution simulation experiments [*Willgoose*, 1989; *Tucker and Bras*, 1998]. Erosion will be less sensitive to hydrology when $M = 1$ instead of $M > 1.5$, and thus erosion and landscape response to changes in hydrology (e.g., climate change, deforestation) will be less severe.

[12] An appropriate sediment transport relationship for steep mountainous settings should characterize the erosion dynamics and accurately predict the spatial and temporal erosion rates. It should also characterize the long-term implications of erosion on landscape evolution such as the concavity of the channel network, its three-dimensional (3-D) texture and terrain properties compared to the observed mountain topography [*Hancock et al.*, 2001]. Thus, for the sediment transport equations developed from flume experiments to be applicable in geomorphologic modeling, they need to be calibrated and revised using field observations on scales relevant to the processes of interest. Long-term implications of selected sediment transport and erosion functions on large-scale landscape evolution need to be tested.

2. Sediment Transport Capacity of Eroding Gullies

2.1. Theory

[13] The dimensionless sediment transport capacity equation (3) is adapted for gully erosion describing basin hydrology and flow hydraulic characteristics as a function of contributing area and slope. Steady state discharge Q is proportional to runoff rate r and contributing area A,

$$Q = rA. \tag{9}$$

Hydraulic radius R is a function of flow cross-sectional area A_f [*Foster et al.*, 1984; *Moore and Burch*, 1986],

$$R = CA_f^{0.5}, \tag{10}$$

where C is a shape constant (see Appendix A). A_f is discharge divided by flow velocity and is estimated as a function of discharge by assuming steady turbulent uniform flow and using Manning's equation for flow velocity. Manning's roughness n is approximated as a function of discharge Q [*Leopold et al.*, 1964; *Knighton*, 1998],

$$n = k_n Q^{-m_n}, \tag{11}$$

where k_n and m_n are empirical parameters. In Manning's equation this gives the flow cross-sectional area as

$$A_f = k_n^{0.75}C^{-0.5}Q^{0.75(1-m_n)}S^{-0.375}. \tag{12}$$

Substituting (12) into (10) gives hydraulic radius as a function of Q and S. Flow cross-sectional area, hydraulic radius, effective shear stress, and flow width are all written

Table 1. Physical Parameters of the Generic Hydraulic Variable Equation, $\Psi = \chi_\Psi Q^{m_\Psi} S^{n_\Psi}$.

ψ	χ_ψ	m_ψ	n_ψ
Flow cross-sectional area, A_f	$k_n^{0.375} C^{-0.5}$	$0.75(1 - m_n)$	-0.375
Hydraulic radius, R	$k_n^{0.375} C^{0.75}$	$0.375(1 - m_n)$	-0.1875
Flow width, W_f	$k_s k_n^{0.375} C^{-0.25}$	$0.375(1 - m_n)$	-0.1875
Effective shear stress, τ_f	$\rho_w g C^{0.75} k_n^{-1.13} n_{gc}{}^{1.5}$	$0.375 + 1.13 m_n$	0.8125

proportional to discharge and slope (Appendices B and C) in the general form (Table 1),

$$\Psi = \chi_\Psi (rA)^{m_\Psi} S^{n_\Psi}, \tag{13}$$

where ψ represents the hydraulic variable of interest and χ_ψ is a constant relating the hydraulic variable to discharge and slope, and m_ψ and n_ψ are theoretically derived exponents (Table 1).

[14] The general sediment transport capacity equation is derived by substituting the shear stress relationship (Table 1) into (4b) and (4b) into (4c), and substituting (4a), (4b), and (4c) into (3) and solving for q_s and finally multiplying q_s with the flow width (Table 1):

$$Q_s = \left[\kappa \chi_c^{-1} \chi_W \chi_\tau^p d^{1.5-p} \left(1 - \tau_c \chi_\tau^{-1} (rA)^{-m_\tau} S^{-n_\tau}\right)^p\right] (rA)^M S^N, \tag{14}$$

where, $\chi_c = \rho_w^p (g(s-1))^{p-0.5}$, $M = pm_\tau + m_W$, and $N = pn_\tau + n_W$. The term in brackets provides the theoretical basis for k_1 in (1) and is independent of discharge when $\tau_c = 0$. This could be a practical assumption for the incision stage of gullies as long as a channel initiation threshold controls gully initiation. The two calibration parameters that appear in the equation are κ and p.

2.2. Calibration Methodology

[15] Sediment transport equations in the form of (3) are often calibrated using data from flume experiments and rivers [*Yalin*, 1977]. In such experiments, parameters κ and p are obtained from q_{s*} and τ_* pairs that are measured throughout the experiments. Here we developed a procedure to obtain the calibration parameters κ and p for gully sediment transport based on Q_{s*} and τ_* pairs estimated from geomorphic field observations in gullies. We measured gully erosion volumes in a mountainous watershed (described later) that was recently gullied due to a thunderstorm whose magnitude and duration are approximately known. We assumed that once a gully was incised the sediment transport rate was at its transport capacity. This transport-limited erosion assumption is consistent with the flume experiments of rills and gullies for cohesionless sediments in the case of unlimited sediment supply [*Cochrane and Flanagan*, 1997; *Bennett et al.*, 2000]. On the basis of this assumption the average unit sediment discharge of a particular flow cross section in the gully can be approximated by the total volume of sediment passing that point V_s (volume of total estimated erosion that originated from the upslope contributing area) divided by the total erosion duration T, and flow width W_f,

$$q_s = \frac{V_s}{TW_f}. \tag{15}$$

Writing W_f as a function of area and slope (13) and substituting (15) into (4a), we obtain the dimensionless sediment transport rate of a particular flow cross section as a function of sediment volume passing that cross section (field observation), upslope contributing area, and the local slope as

$$q_{s*}(V_s, A, S) = \frac{V_s}{T\chi_W (rA)^{m_W} S^{n_W} \sqrt{g(s-1)d^3}}. \tag{16}$$

Similarly substituting the shear stress as a function of area and slope (13) into (4b), we have the dimensionless shear stress described in terms of area and slope

$$\tau_*(A, S) = \frac{\chi_\tau (rA)^{m_\tau} S^{n_\tau}}{\rho_w g(s-1)d}. \tag{17}$$

Now with $p = p_\beta$, equation (4c) in (3) gives

$$q_{s*} = \begin{cases} \kappa\left(\tau_*\left(1 - \tau_{*c}/\tau_*\right)\right)^p & \tau_* > \tau_{*c} \\ 0 & \text{otherwise} \end{cases}. \tag{18}$$

We denote $\tau'_* = \tau_* (1 - \tau_{*}c/\tau_*)$ and obtain the empirical parameters κ and p by plotting the observed q_{s*} versus τ'_* and fitting a power function. This calibration procedure requires field estimates of three spatially distributed quantities (V_s, A, and S) at different points along the gullies, estimates of the other sediment transport model parameters in (14) (see Table 3 below), and the erosion duration T and runoff rate r for the gully incising runoff event. In the following sections we describe our field area and the methods used to estimate these quantities.

3. Field Study

[16] The sediment transport capacity equation described above has been calibrated using field data from the Idaho Batholith region. This region consists of an extensive mass of granitic rock approximately 41,400 km^2 in size that covers a large part of forested, mountainous central Idaho and adjacent Montana. Valleys are typically narrow and V-shaped. Erodible coarse textured soils are found on steep gradients that often exceed 70% [*Megahan*, 1974]. Colluvium that accumulates in hollows and steep headwater channels is episodically evacuated by gullying and debris slides [*Kirchner et al.*, 2001]. Average annual precipitation is approximately 1000 mm. Localized high-intensity rainstorms (25–50 mm/h) of short duration (<0.5 hour) occur during summer. At other times of the year more widespread storms occur, often in conjunction with snowmelt. Following soil disturbance and wildfires, the combination of steep topography, high soil erodibility, and high–intensity summer thunderstorms or rapid snowmelt often results in accelerated surface erosion and landslides [*Megahan and Kidd*, 1972; *Meyer et al.*, 2001].

[17] The specific study area selected is Trapper Creek within the North Fork of the Boise River in southwestern Idaho (see Figure 1). Trapper Creek was intensely burned by a wildfire in 1994, and extreme gullying occurred during a convective summer storm in 1995, due possibly to water-repellent conditions of the surface soil. On the average the gullies were 1–2 m deep and 3–4 m wide. Relatively narrow cross sections were observed at sites where all the colluvium

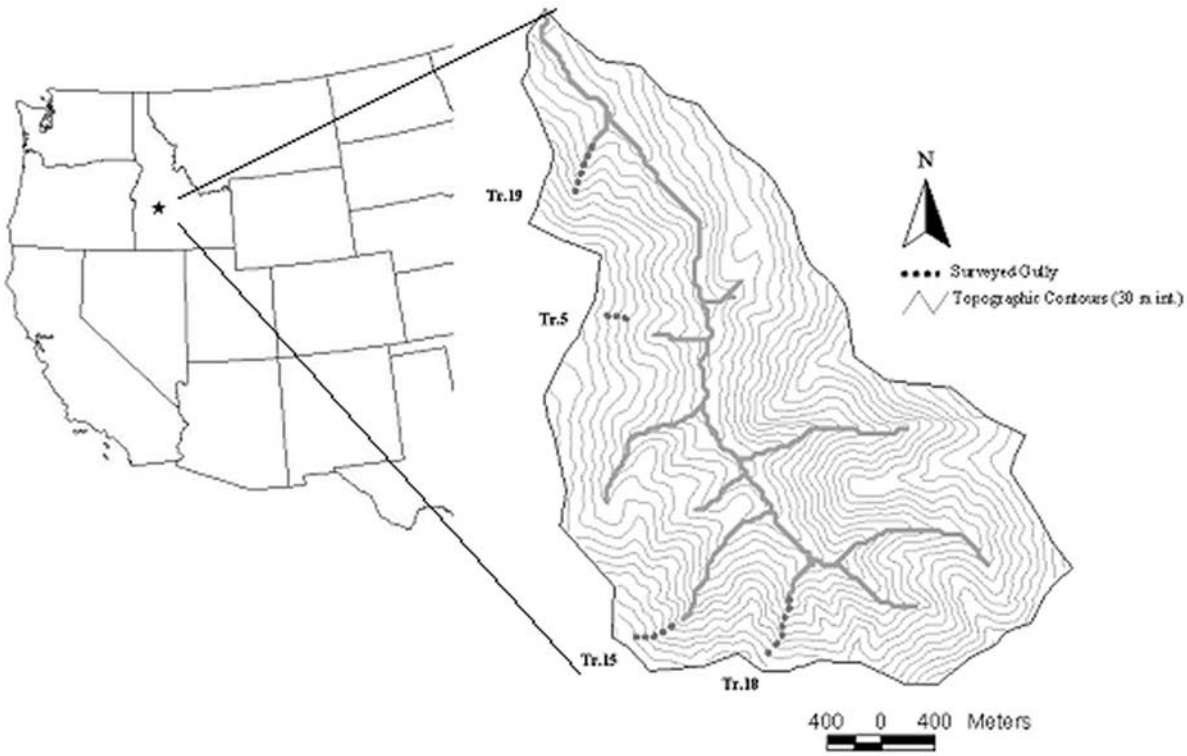

Figure 1. Location map of the study area and the four gullies studied in the field. In the figure, "Tr." is an abreviation for Trapper Creek, and the number following "Tr." is the gully numbered in the field.

was scoured to bedrock. Widening of the gully cross sections was due to sidewall collapse at most of the sites. Cobbles and boulders up to 0.3 m in diameter, which were presumably introduced by sidewall collapse, were deposited downstream of the sidewall failure. Other than these coarse materials no significant deposition was observed in the gullies.

[18] In the field we recorded the locations of channel heads, gully heads, and heads of the continuous gullies. Here channel head refers to the most upstream limit of erosion within definable banks, whereas gully head refers to the sequential head cuts observed downstream from the channel head where gullies were discontinuous. The continuous gully head refers to the head cut below which the gully is continuous. In order to estimate the volume of eroded material from the gullies we estimated the preerosion surface by projecting the side slopes into the eroded gully trough and measured the gully cross-sectional area below this estimated preerosion surface at locations spaced on the average at 30 m. All significant sediment scours observable in the discontinuous gully reaches were also measured. Slope measurements were taken at each measurement location over a length of 10–20 m. This measurement protocol was applied for distances ranging between 150 and 500 m downslope from gully heads in four different gullies including one discontinuous gully. The field data collected are reported in Table 2.

4. Field Estimates for the Parameters of q_{s*} and τ'_*

[19] Gully erosion volumes between successive gully cross sections were calculated by multiplying the distance between the two cross sections by the average cross-sectional area. Total sediment passing a particular cross section, V_s, is then estimated by accumulating all the upslope erosion measurements along the gully profile down to that particular point. Calibration of the sediment transport theory requires two topographic variables, the contributing area and local slope at each measurement location. Slope was measured in the field. Contributing area was derived from the 30 m U.S. Geological Survey (USGS) digital elevation model (DEM) (level 2) of the study site using the D∞ algorithm [*Tarboton*, 1997]. There was a forest road located upslope from the gullies that influenced drainage. We used the mapped road flow directions and road structures to detect road-induced abnormalities. For gully Tr.15 (Figure 2), 25,000 m^2 of additional contributing area was added due to the road drainage from the surrounding hillslopes. The plotting of q_{s*} versus τ'_* described above also requires the estimates of median sediment size of the eroding material d, runoff rate r, erosion duration T, Manning's roughness for grains n_{gc}, parameters k_n and m_n for the total channel roughness estimates from discharge, and channel shape and cross-sectional parameters. All of these parameters could vary in space and time as gullies erode; however, we made estimates based on field observations to characterize the average conditions as described below. The parameters and the basis for their estimation are summarized in Table 3.

[20] We measured an average median sediment size of 2 mm for the surface sediment in Trapper Creek on hillslopes surrounding the gully heads. Sediment sizes visually observed on the gully walls were coarser than a median sediment size of 2 mm due to the increased fraction of

Table 2. Gully Erosion Data Collected in the Study Site

Gully Number	Drainage Area, m^2	Local Slope, m/m	Total Gully Erosion, m^3
Tr.05	5,460	0.36	1.9
	6,690	0.35	16.8
	9,000	0.55	35.7
	9,600	0.55	65.7
	12,000	0.55	103.4
	12,900	0.55	115.3
	16,500	0.28	147.9
	22,500	0.55	196.9
	24,000	0.55	212.4
	27,600	0.53	223.3
	30,000	0.50	240.5
	33,600	0.35	264.0
	34,440	0.33	312.1
Tr15	17,040	0.34	189.5
	18,900	0.39	503.3
	20,880	0.45	573.2
	25,680	0.55	753.2
	30,780	0.50	934.7
	34,950	0.49	987.2
	46,800	0.41	1,089.1
	50,940	0.40	1,323.9
	46,260	0.49	1,671.3
	83,760	0.32	2,760.8
	89,640	0.40	3,589.7
Tr.18	6,300	0.51	0.36
	8,700	0.47	0.44
	9,000	0.61	0.89
	15,660	0.60	2.79
	19,020	0.64	12.29
	22,500	0.65	23.70
	24,000	0.50	34.07
	26,190	0.50	38.87
	42,000	0.60	58.87
	45,300	0.40	95.77
	61,620	0.4	178.27
	69,900	0.44	358.27
	74,880	0.43	478.27
	81,000	0.35	652.27
	100,200	0.29	936.27
	102,000	0.29	1,126.27
	107,130	0.3	1,696.27
	115,860	0.37	2,576.27
	135,000	0.3	3,176.27
	158,430	0.28	3,921.27
	210,000	0.2	4,946.27
	253,680	0.13	6,096.27
	268,890	0.24	7,176.27
	276,000	0.24	8,046.27
Tr.19	18,000	0.45	16.5
	38,610	0.48	33.5
	46,800	0.46	67.0
	54,000	0.45	116.5
	60,000	0.4	144.0
	74,550	0.4	171.5
	87,000	0.35	177.6
	90,000	0.35	207.2
	94,260	0.45	248.2
	120,000	0.32	273.2
	125,790	0.31	299.7
	150,000	0.18	418.4
	156,480	0.19	572.4
	166,740	0.2	604.2
	188,070	0.18	624.4
	198,750	0.17	633.9
	210,000	0.16	680.3
	216,480	0.2	708.5
	222,000	0.18	827.5
	228,000	0.23	887.0

gravel. Published studies [*Megahan*, 1992; *Gray and Megahan 1981*; *Meyer et al.*, 2001] that have examined sediment size in the Idaho Batholith all report that median sediment size is typically in the range of coarse sand and fine gravel. Therefore we used a median sediment size of 3 mm for gully sediment transport.

[21] We used a commonly accepted value of 0.045 [*Suszka*, 1991] for the dimensionless critical shear stress for incipient motion, τ_{*c}. This value is consistent with the τ_{*c} values reported by *Buffington and Montgomery* [1997] for coarse sand and fine gravel. Under the high shear stresses common on steep slopes the choice of τ_{*c} does not have very much influence on sediment transport.

[22] Although the rainfall rate of the storm that incised the channels in Trapper Creek was not measured, Forest Service personnel exposed to the storm estimated that more than an inch of rain fell in less than half an hour. The nearby Prairie rain gage has 35 mm for the largest 30-min event in a 23-year record, i.e., a rate of 70 mm/h. We assumed that the Trapper event was of this order of magnitude and selected a steady state runoff rate of 35 mm/h assuming about 50% infiltration due to the water repellency remaining a year after the wildfire. This information was also the basis for the estimate of the uniform probability distribution for instantaneous runoff rates used by *Istanbulluoglu et al.* [2002] to calculate the probability of channel initiation for the same event in Trapper Creek. Using different runoff rates in the calibration affects the κ constant slightly but has no influence on the shear stress exponent p. In the area, convective summer storms often last less than or approximately half an hour. We assumed that all the gully incisions occurred in $T = 0.5$ hour.

[23] Grain roughness (n_{gc}) for fine gravel is selected as 0.025 [*Chow*, 1959; *Arcement and Schneider*, 1984]. The at-a-station Manning's roughness relationship (equation (11)) gives total roughness n as a function of parameters k_n, m_n, and discharge, which in our case is obtained from runoff rate and contributing area [*Leopold et al.*, 1964; *Knighton*, 1998]. In Tr.19 we observed small boulders up to 300 mm in diameter, exposed rocks on the sides of the channel, and logs at several locations along the gully channel. On the basis of these observations we rated the degree of irregularity of the channel and the effects of obstructions as "severe" for the gully-incising event. Additional Manning's roughness values n_{ac} for such conditions can be in the range of 0.05–0.1 [*Chow*, 1959; *Arcement and Schneider*, 1984], which yields total roughness, $n = n_{gc} + n_{ac}$, in the range 0.075–0.125. In the surveyed sections of Tr.19 the discharge is calculated to be in the range 0.15–1.9 m^3/s. We therefore estimated k_n = 0.08 in equation (11) to match this total roughness range. We took k_n = 0.045 for the rest of the gullies (Tr.5, Tr.15, Tr.18) where channels were relatively clear of obstructions. This results in additional roughness values in the range of 0.015–0.055 for the calculated discharge range of 0.05–2.2 m^3/s. This range corresponds to moderate to severe effect of obstructions for the gully-incising event [*Chow*, 1959; *Arcement and Schneider*, 1984]. The field observed gully width to depth ratio was roughly 2, and gully cross sections could be considered to be roughly parallel. A parabolic flow cross section with a width to depth ratio of 2 was used to obtain the shape parameters

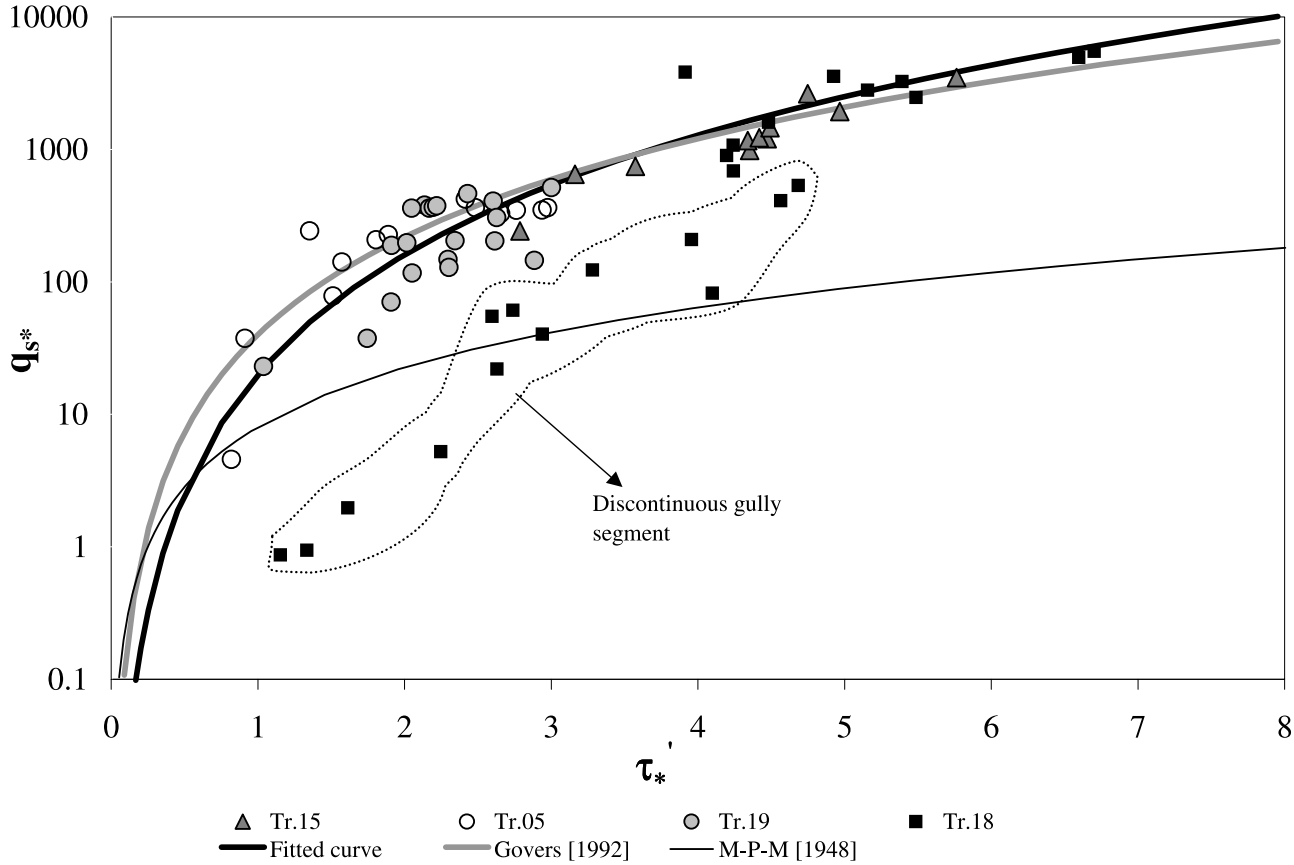

Figure 2. Relationship between q_{s*} and τ_*' obtained using the field observations. The solid lines are fitted power relationships in the form of equation (3).

C and k_s used to calculate the flow width and shear stress in eroding gullies.

[24] The area and slope exponents for shear stress (m_τ = 0.6, n_τ = 0.8125) and the flow width (m_w = 0.3, n_w = −0.1825) are calculated using the expressions derived in Appendices B and C and given in Table 1 with a selected m_n = 0.2 [*Knighton*, 1998].

[25] The presence of sediment at high concentrations in the flow may change the fluid properties, decrease the flow velocity, and increase its depth [*Aziz and Scott*, 1989]. As the sediment concentration increases, flow hydraulics becomes much more complicated compared to clear water flow due to the interactions among solid particles [*Hashimoto*, 1997; *Jan and Shen*, 1997]. There is theoretical and experimental evidence, however, that even debris flows can be regarded as a special type of flow that can be described by similar hydraulic formulations such as Manning's and Chezy's equations for flow velocity [*Rickenmann*, 1999]. In this paper, flow velocities and shear stresses are calculated assuming the hydraulic properties of clear water flow.

5. Results and Discussions

[26] The relationship between q_{s*} and τ_*' obtained using the field data is presented in Figure 2. The figure also plots the fitted power function relationship in the form of (3) with κ = 20 and p = 3. The Meyer-Peter Muller and Govers sediment transport relationships were also plotted on Figure 2 for comparison with the fitted relationship. Details of these equations are given below. All the data points except for the first 13 points of Tr.18 show good correspondence with the theoretical derivations.

[27] The major sources of sediment discharge in gullies are sediment detachment from the bed, widening by under-

Table 3. Parameters Used in the Estimation of Dimensionless Sediment Flux and Dimensionless Shear Stress

Parameter	Value	Basis
d	3	field observations and literature
τ_{*c}	0.045	*Suzka* [1991]
r	35 mm/h	field estimate; *Istanbulluoglu et al.* [2002]
T	0.5 h	field estimate
n_{gc}	0.025	fine gravel; *Chow* [1959], *Arcement and Schneider* [1984]
k_n	0.08, 0.045	estimated to match field roughness range with calculated discharge range
m_n	0.2	*Knighton* [1998]
C	0.346	equation (A4) with z_1 = 2
k_s	1.73	Appendix C for parabolix channels with z_1 = 2
m_τ	0.6	Appendix B with m_n = 0.2
n_τ	0.8125	Appendix B
m_w	0.3	Appendix C with m_n = 0.2
n_w	−0.1825	Appendix C
g	9.81 m/s^2	physical constant
s	2.65	quartz specific gravity
ρ_w	1000 kg/m^3	physical constant

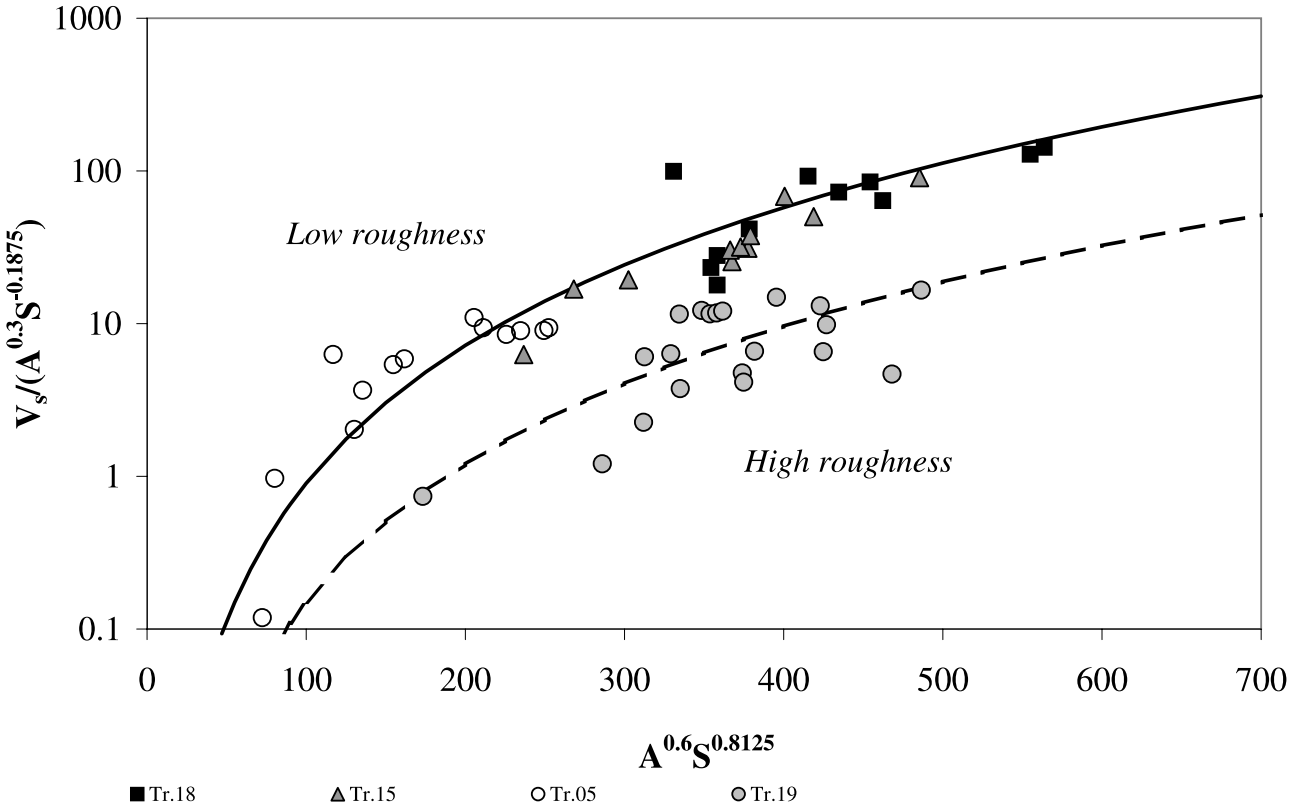

Figure 3. Field observations of $V_s/A^{0.3}S^{-0.1875}$ used as a surrogate for sediment discharge versus $A^{0.6}S^{0.8125}$ used as a proxy for shear stress.

cutting, and side-slope failures [*Selby*, 1993]. In Figure 2, thirteen data points (circled by dashed line) from gully Tr.18 fall significantly below the trend of the fitted dimensionless sediment transport capacity curve. The first four data points represent the sediment transport in the first 60 m of the gully reach starting from the channel head that has two discontinuous channel segments each about 30 m long and 5–20 cm deep. No side-slope failures were observed, and sediment input to the flow was presumably due to sediment detachment from the bed and partly from the walls of the channels. Downslope of the discontinuous channel segment the gully is continuous and incision depths start increasing abruptly and reach to about 1.20 m at about 120 m downslope from the channel head. Beyond this point side-slope failures were observed at short intervals. Presumably these subsequent side failures supplied considerable sediment to the flow, which reached its transport capacity (Figure 2). The growth of Tr.18 was evidently slower than the other gullies where significant scour was observed in relatively short distances. Since the $q_{s*} - \tau'_*$ pairs plotted in Figure 2 were calculated assuming channeled sediment transport, it is consistent that detachment around the flow cross section and supply-limited channel segments would plot below the transport capacity relationship.

[28] The dimensionless shear stress exponent p we found is consistent with the total load equations in the form of (3). The theory uses spatially distributed observations of gully erosion volumes, drainage areas, and slopes and assumes that the rest of the model inputs are spatially constant. Therefore q_{s*} and τ^* used in Figure 2 (equations (16) and (17)) are scaled quantities of the field observations as

$$q_{s*} \propto \frac{V_S}{A^{m_w} S^{n_w}} \tag{19}$$

$$\tau_* \propto A^{m_\tau} S^{n_\tau}. \tag{20}$$

The fitted exponent p is therefore insensitive to the uncertainties in the parameters used in nondimensionalizing these quantities, while the coefficient κ is sensitive to parameter uncertainty. However, the κ value we found (Figure 2) using the reported parameters (Table 3) is in the range of the κ values reported in the literature [*Simons and Senturk*, 1977; *Garde and Raju*, 1985]. Figure 3 plots direct field observations of $V_s/A^{0.3}S^{-0.1875}$ used as a surrogate for sediment discharge, versus $A^{0.6}S^{0.8125}$ used as a proxy for shear stress. A power relationship with an exponent $p = 3$ has been fit to this data,

$$\frac{V_s}{A^{0.3}S^{-0.1875}} \propto \left(A^{0.6}S^{0.8125}\right)^3. \tag{21}$$

The outliers in Figure 2 were excluded from the plot since the tested theory is for sediment transport capacity conditions. Except for Tr.19, where rougher channel conditions were observed, the data plot close to the same curve (solid line in Figure 3). Tr.19 data plot below the rest of the data but shows the same functional form (21) (dashed line). When the roughness of Tr.19 is character-

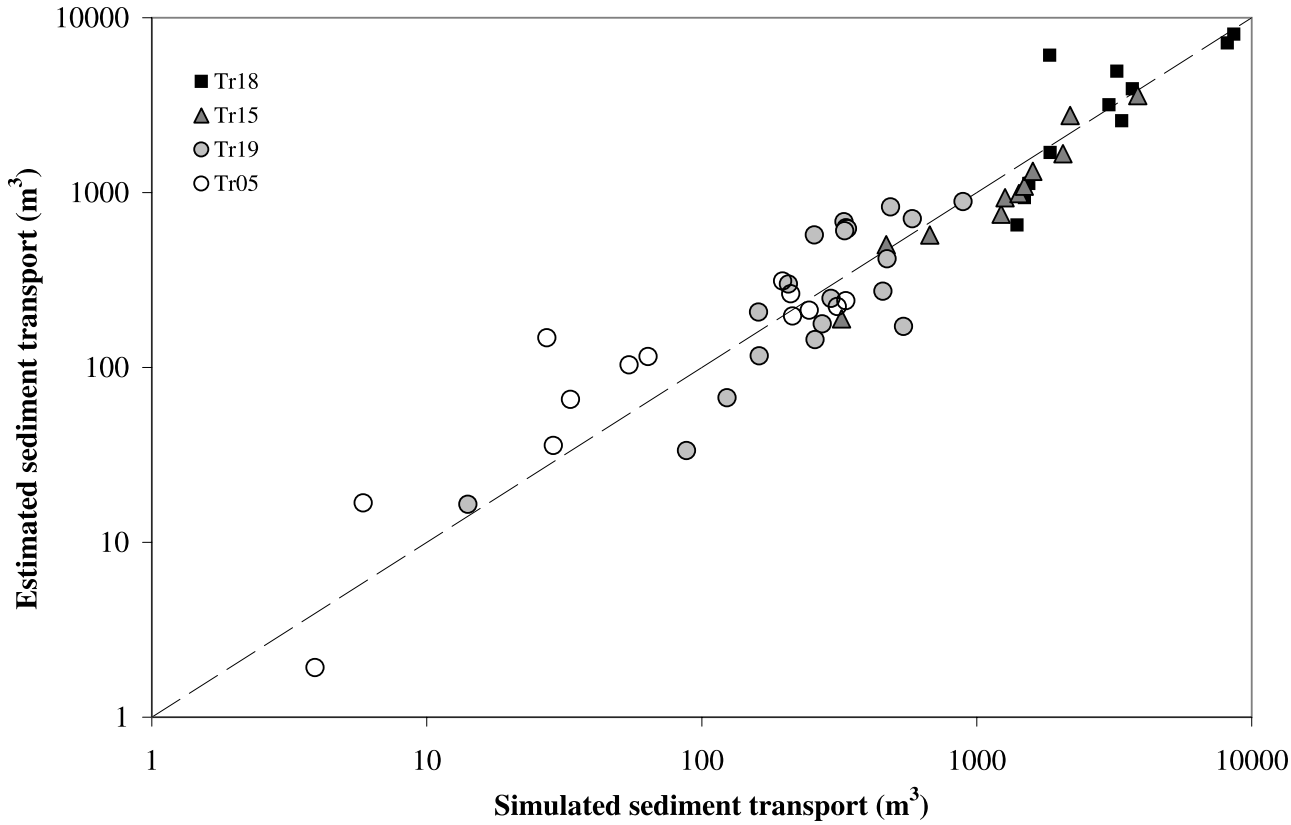

Figure 4. Comparison of the calculated sediment transport using the calibrated model parameters of κ = 20 and p = 3 to the estimated sediment transport in the field. For the combined data for gullies Tr.05, Tr.15, and Tr.18, R^2 = 0.84 and NS = 0.83. For the Tr.19 data set alone, R^2 = 0.5, NS = 0.44.

ized with a higher constant, all the data collapse on to one functional relationship equation (3) (Figure 2). Figure 3 shows the field evidence that sediment transport capacity on steep gullies is a nonlinear function of shear stress with p = 3. Figure 3 also indicates that sediment transport capacity is reduced with the rougher conditions observed in Tr.19. This is theoretically described in equations (B3)(B6)–(B7), which show that as the total roughness coefficient increases due to additional roughness elements such as nontransportable grains and obstructions, the fraction of the shear stress acting on transported grains decreases and reduces the sediment transport rate.

[29] In many hillslope erosion models [*Lane and Nearing*, 1989; *Woolhiser et al.*, 1990; *Coulthard et al.*, 2000] the transport capacity of overland and rill flows is represented by adopting existing bed load equations developed from observations of alluvial rivers and channels [*Julien and Simons*, 1985]. The hydraulic conditions of shallow flows on steep slopes can be different from much deeper channel flows [*Abrahams and Parsons*, 1991; *Ferro*, 1998]. *Govers* [1992] tested the performance of a number of bed load equations using his data set obtained simulating rill flow on slopes ranging from 1.7% to 21% in a laboratory flume and other data sets giving the sediment transport capacity of overland flow. He found that bed load equations are inappropriate for overland flow on slope ranges steeper than they were originally developed. He suggested that overland flow does not necessarily show a bed-load-type transport behavior and that the shear stress exponent p in (2) should be ~2.5 for the transport capacity of shallow flows on steep slopes. In Govers's equation, the exponent p = 2.5 therefore accounts for both suspended and bed load transport. In order to test Govers's conclusions, we compared the Meyer-Peter and Muller and Govers sediment transport equations with our data by plotting their dimensionless forms in Figure 2. In the Meyer-Peter and Muller bed load equation, κ = 8 and p = 1.5. The *Govers* [1992] equation has the form of (2) and is not consistent for nondimensionalization in the form of equation (3), unless κ is written as a function of sediment size and sediment specific gravity as for clear water as the transporting fluid (see Appendix D).

[30] When the ($\tau'_* - q^*$) curve for the Meyer-Peter and Muller equation is compared to the data, one can see that classical bed load equations with p = 1.5 would significantly underpredict sediment transport on very steep slopes at high shear stresses. Bed load equations for alluvial rivers such as the Meyer-Peter and Muller equation were tested for slopes in the range of 0.1% up to 2% and in the τ_* range of 0.1–1. They often give good results in the slope range of 0.1–0.3% [*Yalin*, 1977]. Therefore high flow shear stresses on steep slopes are significantly above their test range. This comparison allows us to visualize how a hillslope erosion model using a generic bed load equation may underpredict sediment transport in rills and gullies [*Foster et al.*, 1989].

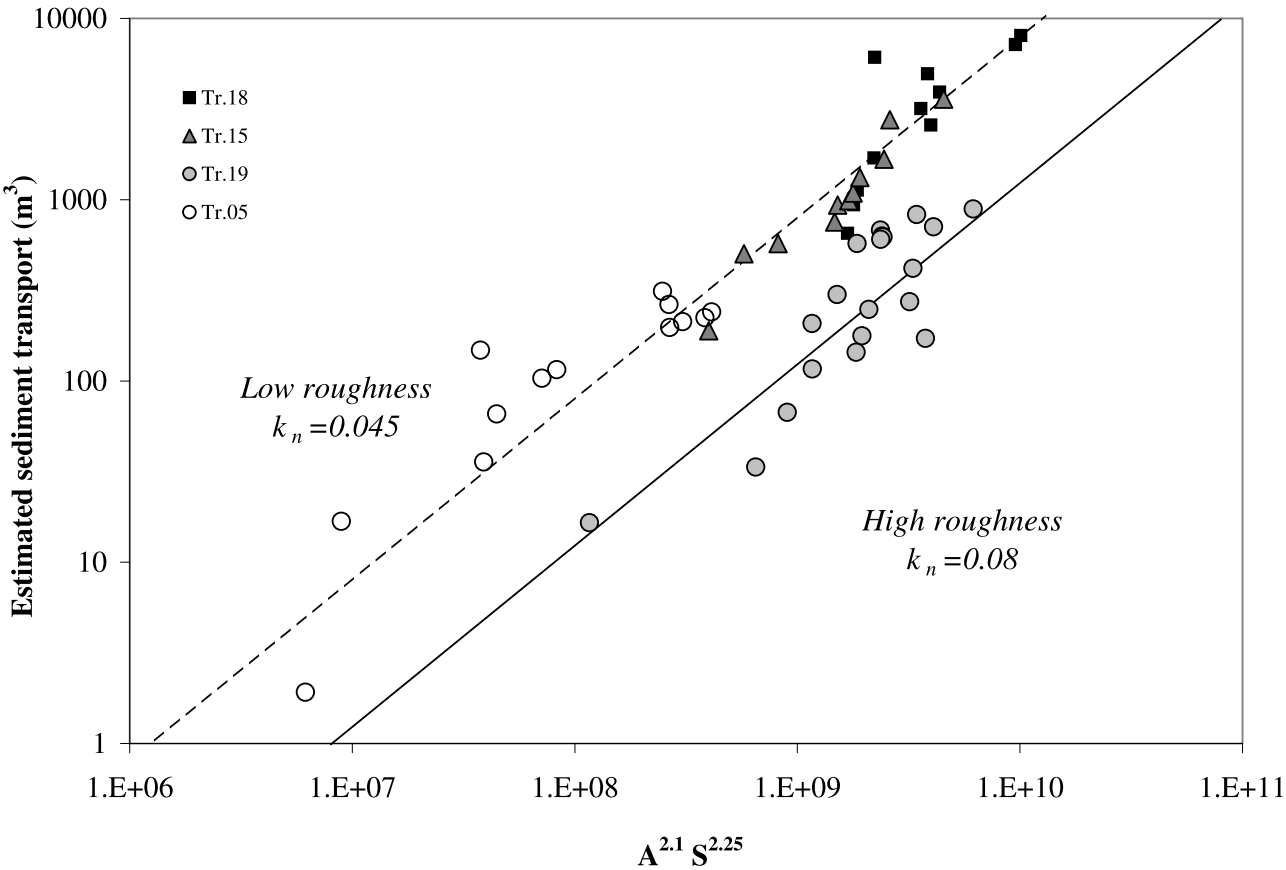

Figure 5. Estimated sediment transport as a function of contributing area and slope using their derived exponents at surveyed gully segments. The lines plot equation (14). The solid line is for $k_n = 0.08$, which is for higher roughness conditions observed in Tr.19, and the dashed line is for $k_n = 0.045$ for the rest of the gullies.

In distributed models, such mispredictions may not be detected since models are often calibrated optimizing several parameters using basin outlet data. However, biased spatially distributed erosion estimates may severely affect spatial model results. The dimensionless form of the Govers equation for shallow overland and rill flow for steep slopes corresponds well with the field data.

[31] Figure 4 plots the total sediment transport volumes calculated from equation (14) with the derived exponents $M = 2.1$ and $N = 2.25$ (based on $p = 3$, $m_\tau = 0.6$, $n_\tau = 0.8125$, $m_w = 0.3$, $n_w = -0.1825$, and $m_n = 0.2$) against the estimated volumes in the field. The outliers in Figure 2 were excluded from the plot. Regression coefficients (R^2) and Nash-Sutcliffe error measures (NS) [e.g., *Gupta et al.*, 1998]

$$NS = 1 - \frac{\sum (Q_s T - V_s)^2}{\sum (V_s - \overline{V}_s)^2} \tag{22}$$

are calculated for each group of gullies where the model inputs were selected constant. According to equation (14), spatially constant model parameters imply that $Q_s = const. A^{2.1} S^{2.25}$. The combined data from Tr.05, Tr.15, and Tr.18 revealed both R^2 and NS equal to 0.83, indicating that 83% of the spatial variability of the sediment transport rates can be represented by the model. For Tr.19 we obtained $R^2 = 0.5$ and $NS = 0.44$. This means that only 44% of the variability of the sediment transport rates over the terrain can be represented by the model. In the field we observe more logs, boulders, and exposed bedrock in Tr.19 than in the other three gullies. We infer that the exposed rock and additional variability in roughness limits entrainment and leads to a significantly lower performance of the model using spatially constant roughness values in Tr.19.

[32] To show the relationship between topography and sediment transport, we plotted the estimated sediment transport volumes in the field as a function of $A^{2.1}S^{2.25}$ (Figure 5) along with equation (14) using the field estimates of the model inputs.

[33] Topographic concavity expresses the long-term effects of sediment transport and provides another check on sediment transport functions. If the sediment transport function that we calibrated using field data is valid over the long term, then the concavity index calculated using the calibrated exponents M and N (equation (5)) should be consistent with the index that can be inferred from the data. Figure 6 plots the local slope versus contributing area observed along gully profiles at each measurement location. Lines are the power law relationships between area and slope that characterize the hillslope profile concavity (equation (5)). They are plotted as the upper and lower bounds of the data points which show an inverse relationship between

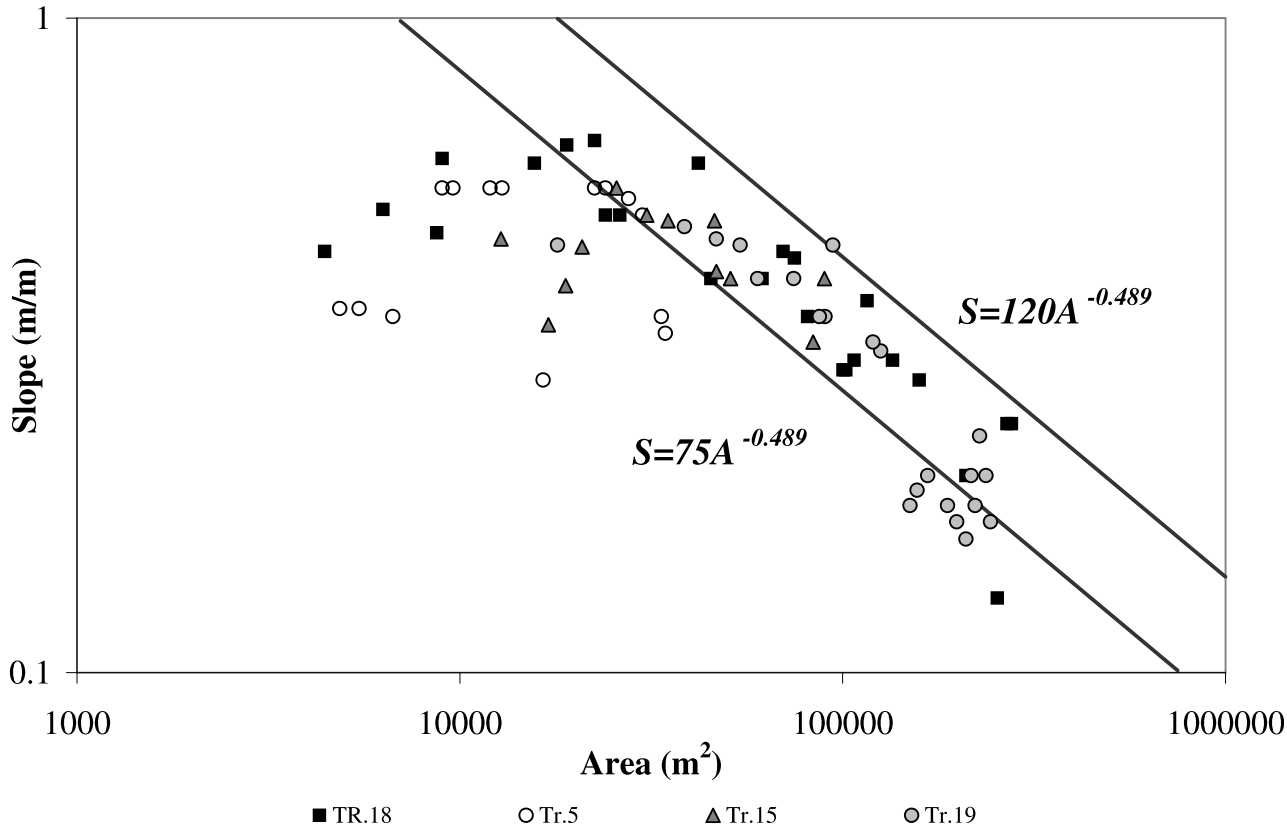

Figure 6. Slope-area plot of the gully profiles observed in the field. Lines are the power law relationships of the profile concavity between area and slope (equation (3)) plotted as the upper and lower bounds of the data that show an inverse relationship between slope and area. M = 2.1 and = 2.25.

slope and area. The concavity index is calculated using the area and slope exponents M = 2.1 and N = 2.25 of the sediment transport relationship. This figure implies that the form of the sediment transport equation derived using field data from a single gully-forming event may be consistent with the fluvial transport processes acting over the long term. Note that data points where a positive relationship between area and slope is observed presumably lie on the hillslopes where slope forming diffusion sediment transport dominates incisive gully erosion. Therefore they are not considered in the analysis.

6. Conclusions

[34] Sediment transport capacity is often parameterized as a nonlinear function of shear stress or interchangeable discharge or contributing area and slope in theoretical geomorphology. Although extensive data sets exist that decipher the nonlinearity in relationships between sediment transport and shear stress, discharge and slope (equations (1) and (2)) in experimental flume scales, we know of no study that examines the theoretical foundations of these equations for naturally eroded gullies surveyed in the field. In this paper we adapted a generic dimensionless sediment transport function (3) to incision of gullies on steep slopes by describing the hillslope hydrology and flow hydraulics based on contributing area and local slope. We calibrated the parameters of the dimensionless sediment transport function, an empirical constant κ, and a shear stress exponent p for the case of recent gully erosion using field data from a steep, burned mountainous basin in southwestern Idaho, United States.

[35] Our field data suggested that under high shear stresses, p = 3. This exponent is twice the shear stress exponents used in classical bed load equations but consistent with total load equations [*Garde and Raju*, 1985]. *Engelund and Hansen* [1967] noted that starting from the incipient motion of bed load the τ_* exponent increases from 1.5 to 2.5 and even up to 3 under high shear stresses in equation (3) as the flow intensity and the suspended load movement increases [*Chien and Wan*, 1999]. Bed and total load equations were mostly developed for alluvial rivers with gentle slopes and bed forms, and under relatively lower τ_* ranges than we calculated for our gullies. Thus their applicability on steep hillslopes can be questionable. However, Govers's flume experiments on steep slopes with well-sorted mixtures also reveal a shear stress exponent p = 2.5 and show good correspondence with the field data (Figure 2). We suggest that sediment transport capacity of incising gullies can be modeled using equation (14) with either the model calibration parameters obtained in this study or the parameters derived from the Govers equation.

[36] The model driven by spatially constant inputs represents 83% of the spatial variability of the sediment transport rates in gullies Tr.05, Tr.15, and Tr.18 located in three different hollows. The reason for this good performance is attributed to the rather spatially homogenous model inputs such as the sediment sizes and the roughness conditions

observed in these gullies. For the case of Tr.19 the model explains only 44% of the spatial variability of the sediment transport rates. We infer that the reason for a significantly lower model performance in Tr.19 is due to the heterogeneities in the roughness conditions and exposed rock that are not spatially characterized in the model.

[37] The shear stress exponent $p = 3$ theoretically corresponds to exponents $M = 2.1$ and $N = 2.25$ in the sediment transport equation (1) that has been plotted in Figure 5. This plot shows the importance of topography in concentrated erosion. In the literature several M and N exponents have been presented for different sediment transport processes such as creep, soil wash, and rivers [*Kirkby*, 1971; *Arrowsmith et al.*, 1996]. For soil wash and gullying, reported values of area and slope exponents are in the range of $M = 1–2$ and $N = 1.3–2$. The exponents we find are higher than the upper limit of these published values. In the literature, however, contributing area is represented as the specific catchment area (contributing area per unit contour width) instead of contributing area concentrated in a gully, and the exponents were empirically developed based on longer observation periods.

[38] One of the implications of the sediment transport function on landscape morphology is the concavity of the channel network. The concavity index $\theta_c = (M - 1)/N$ obtained from the area and slope exponents of the sediment transport equation agree well with the observed profile concavity of the gullies. This shows that the sediment transport equation developed using a single erosion event is consistent with the functional form of sediment transport over the long term.

Appendix A: Derivation of the Shape Constant C for Trapezoidal, Triangular, and Parabolic Channels

[39] The shape constant in equation (10) is given here for trapezoidal, triangular, and parabolic channels based on the width to depth ratio z_1 and sideslope ratio z_2 (for triangular and trapezoidal channels only). We recognize that for a fixed channel z_1 changes with discharge (and depth); nevertheless it is treated here as a constant parameterization of the form of an eroding channel where there is some degree of adjustment of cross-sectional form to discharge. Equation (10) gives

$$C = \frac{A_f^{0.5}}{R}. \tag{A1}$$

Writing A_f and R as a function of z_1 and z_2, we obtain C_s for trapezoidal, triangular, and parabolic channel geometries from (A1) respectively;

$$C_{trap} = \frac{(z_1 - z_2)^{0.5}}{(z_1 - 2z_2) + 2\left(z_2^2 + 1\right)^{0.5}} \tag{A2}$$

$$C_{tri} = \frac{z_2^{0.5}}{2\left(z_2^2 + 1\right)^{0.5}} \tag{A3}$$

$$C_{prb} = \frac{\sqrt{1.5}z_1^{1.5}}{1.5z_1^2 + 4}. \tag{A4}$$

Appendix B: Derivation of the Effective Shear Stress Proportional to Q and S

[40] It is commonly assumed in sediment transport mechanics that both the Manning's roughness coefficient and hydraulic radius are the summation of those of grains and bed forms [*Simons and Senturk*, 1977]. Here we assumed that (1) bed form resistance is negligible during gully incision and (2) nontransportable obstacles and gully shape irregularities impose additional resistance to the flow similar to bed forms. Manning's equation for open channel flow gives

$$V = \frac{R^{2/3}S^{1/2}}{n}, \tag{B1}$$

where n is the Manning's roughness coefficient. The total shear stress at the channel bed is

$$\tau = \rho_w gRS. \tag{B2}$$

Manning's roughness is composed of a grain and additional roughness components,

$$\mathrm{n} = n_{\mathrm{gc}} + n_{ac}. \tag{B3}$$

Given an average flow velocity in the channel, the grain component of hydraulic radius is obtained as [*Laursen*, 1958]

$$R_{gc} = \left(n_{gc}\frac{V}{S^{0.5}}\right)^{1.5} \tag{B4}$$

from (B1) with only the grain roughness considered. This is then assumed to give the effective shear stress acting on grains in (B2) as

$$\tau_f = \rho_w gR_{gc}S. \tag{B5}$$

Substituting (B1) into (B4), R_{gc} is written as a function of R,

$$R_{gc} = R\left(\frac{n_{gc}}{n}\right)^{1.5}. \tag{B6}$$

Equation (B6) predicts grain hydraulic radius as a fraction of the total hydraulic radius.

[41] Observations in rivers have revealed an inverse relationship between Manning's roughness coefficient and discharge at a given station, because as flow depth increases roughness elements become relatively less effective in retarding the flow [*Dingman*, 1984]. Here we implemented an empirical relationship for n based on discharge [*Leopold et al.*, 1964; *Knighton*, 1998],

$$\mathrm{n} = k_n Q^{-m_n}, \tag{B7}$$

where k_n and m_n are empirical parameters. Equation (B7) when substituted into (B6) predicts an increase in $(n_{gc}/n)^{1.5}$ with discharge, which suggests that as discharge increases the fraction of the grain hydraulic radius would increase. Now equation (12) is substituted into equation (10). The result and equation (11) are substituted into equation (B6) to

get R_{gc}. R_{gc} is substituted into equation (B5) to finally arrive at

$$\tau_f = \rho_w g k_n^{-1.13} C_s^{0.75} n_{gc}^{1.5} Q^{0.375+1.13m_n} S^{0.8125}. \quad \text{(B8)}$$

Appendix C: Derivation of the Flow Width in an Eroding Channel Proportional to *Q* and *S*

[42] Given the assumption of a constant width to depth ratio of the flow in an eroding channel, the flow cross-sectional area can be described by W_f, z_1, and z_2 for different channel geometries. The flow cross-sectional areas of trapezoidal, triangular, and parabolic channels are obtained as

$$A_{f,trap} = \frac{W_f^2}{z_1} - \frac{W_f^2 z_2}{z_1^2} \quad \text{(C1)}$$

$$A_{f,tri} = \frac{W_f^2}{4z_2} \quad \text{(C2)}$$

$$A_{f,prb} = \frac{2W_f^2}{3z_1}. \quad \text{(C3)}$$

Equating (12) to A_f described by channel geometry above and solving for W_f, we obtained the flow width as a function of Q and S,

$$W_f = k_s k_n^{0.375} C^{-0.25} Q^{0.375(1-m_n)} S^{-0.1875}, \quad \text{(C4)}$$

where k_s is another dimensionless shape constant which is $z_1/(z_1 - z_2)^{0.5}$ for trapezoidal channels, $2z_2^{0.5}$ for triangular channels, and $(1.5z_1)^{0.5}$ for parabolic channels.

Appendix D: Nondimensional Form of the Govers Equation

[43] An empirical sediment transport equation was proposed by *Govers* [1992] using 434 data points collected from a 6-m-long and 0.117-m-wide nonrecirculating flume. In the experiments the slopes ranged from 1.7% to 21%, and five well-sorted quartz materials with median grain sizes ranging from 0.058 to 1.098 mm were used as sediment. The equation Govers fitted is

$$\log\ T_c = 2.457\ \log\left(\frac{\tau - \tau_c}{d^{0.33}}\right) - 4.348, \quad \text{(D1)}$$

where T_c is the sediment transport capacity in kg m^{-1} s^{-1}. Rearranging this equation, the following expression for the unit sediment discharge q_s (m^3 s^{-1} m^{-1}) is obtained:

$$q_s = \frac{10^{-4.348}}{\rho_s d^{0.811}} \tau^{2.457} \left(1 - \frac{\tau_c}{\tau}\right)^{2.457}. \quad \text{(D2)}$$

This equation is of form similar to equation (3), as can be seen by substituting (4a), (4b), and (4c) into (3) with $p = p_\beta$, and solving for q_s,

$$q_s = \frac{\kappa\sqrt{g(s-1)d^3}}{[\rho_w g(s-1)d]^p} \tau^p \left(1 - \frac{\tau_c}{\tau}\right)^p. \quad \text{(D3)}$$

Equation (D3) is another expression of the generic sediment transport equation that was expressed in dimensionless form in equation (3). Since equations (D2) and (D3) are in the same form, (D3) can be calibrated to (D2). The exponent p is equated to 2.457, and κ is obtained by equating the first terms in (D2) and (D3) and solving for κ,

$$\kappa_G = 10^{-4.348} \rho_s^{-1} \rho_w^{2.457} g^{1.957} (s-1)^{1.957} d^{0.146}. \quad \text{(D4)}$$

The subscript G in κ_G indicates Govers coefficient κ. This equation can be simplified to $\kappa_G = 34.70(s-1)^{1.957} d^{0.146}$ by substituting $\rho_s = 2650$ kgm^{-3}, $\rho_w = 1000$ kgm^{-3}, and $g = 9.81$ m s^{-2}. The calibrated κ and p allow one to write the Govers equation in the form of (3),

$$q_s* = \kappa_G \left(1 - \frac{\tau_{*c}}{\tau_*}\right)^{2.457} \tau_*^{2.457} \quad \text{(D5)}$$

[44] Figure 2 plots this equation to compare with the field observations.

[45] **Acknowledgments.** We are greatly appreciative of financial support from the U.S. Department of Agriculture under contract 9901085 awarded through the Water Resources Assessment Protection Program of the National Research Initiative Competitive Grants Program. We thank field technicians Tom Black and Bernie Riley. We are grateful to Gary Parker for his invaluable comments on the sediment transport theory. We appreciate the thoughtful reviews by Grant Meyer and an anonymous reviewer.

References

Abrahams, A. D., and A. J. Parsons, Resistance to overland flow on desert pavement and its implications for sediment transport modeling, *Water Resour. Res.*, *27*(8), 1827–1836, 1991.

Arcement, G. J. J., and V. R. Schneider, Guide for selecting Manning's roughness coefficients for natural channels and floodplains, *U. S. Geol. Surv. Rep., RHWA-TS-84-204*, 50 pp., 1984.

Arrowsmith, J. R., D. D. Pollard, and D. D. Rhodes, Hillslope development in areas of active tectonics, *J. Geophys. Res.*, *101*(B3), 6255–6275, 1996.

Aziz, N. M., and D. E. Scott, Experiments on sediment transport in shallow flows in high gradient channels, *Hydrol. Sci. J.*, *34*, 465–479, 1989.

Band, L. E., Grain size catenas and hillslope evolution, *Catena Suppl.*, *17*, 167–176, 1990.

Bathurst, J. C., W. H. Graf, and H. H. Cao, Bedload discharge equations for steep mountain rivers, in *Sediment Transport in Gravel Bed Rivers*, edited by C. R. Thorne et al., pp. 453–477, John Wiley, New York, 1987.

Bennett, S. J., J. Casali, K. M. Robinson, and K. C. Kadavy, Characteristics of actively eroding ephemeral gullies in an experimental channel, *Trans. ASAE*, *43*(3), 641–649, 2000.

Buffington, J. M., and D. R. Montgomery, A systematic analysis of eight decades of incipient motion studies, with special reference to gravel-bedded rivers, *Water Resour. Res.*, *33*(8), 1993–2029, 1997.

Burkard, M. B., and R. A. Kostaschuk, Initiation and evolution of gullies along the shoreline of Lake Huron, *Geomorphology*, *14*, 211–219, 1995.

Cannon, S. H., E. R. Bigio, and E. Mine, A process for fire-related debris flow initiation, Cerro Grande fire, New Mexico, *Hydrol. Processes*, *15*, 3011–3023, 2001.

Chien, N., and Z. Wan, *Mechanics of Sediment Transport*, 913 pp., Am. Soc. of Civ. Eng., Reston, Va., 1999.

Chow, V. T., *Open Channel Hydraulics*, McGraw-Hill, New York, 1959.

Cochrane, T. A., and D. C. Flanagan, Detachment in a simulated rill, *Trans. ASEA*, *40*(1), 111–119, 1997.

Coulthard, T. J., M. J. Kirkby, and M. G. Macklin, Modelling geomorphologic response to environmental change in an upland catchment, *Hydrol. Processes*, *14*, 2031–2045, 2000.

Croke, J., and S. Mockler, Gully initiation and road-to-stream linkage in a forested catchment, southeastern Australia, *Earth Surf. Processes Landforms*, *26*, 205–217, 2001.

Dingman, S. L., *Fluvial Hydrology*, 383 pp., W. H. Freeman, New York, 1984.

Englund, F., and E. Hansen, *A Monograph on Sediment Transport in Alluvial Streams*, 62 pp., Teknisk Vorleg, Copenhagen, Denmark, 1967.

Everaert, W., Emprical relations for sediment transport capacity of interrill flow, *Earth Surf. Processes Landforms*, *16*, 513–532, 1991.

Ferro, V., Evaluating overland flow sediment transport capacity, *Hydrol. Processes*, *12*, 1895–1910, 1998.

Foster, G. R., L. F. Huggins, and L. D. Meyer, A laboratory study of rill hydraulics: I. Velocity relationships, *Trans. ASCE*, *27*(3), 790–796, 1984.

Foster, G. R., L. J. Lane, M. A. Nearing, S. C. Finkner, and D. C. Flanagan, Erosion component, in *USDA-Water Erosion Prediction Project: Hillslope Profile Model Documentation*, edited by L. J. Lane and M. A. Nearing, *NSERL Rep. 2*, pp. 10.1–10.12, Natl. Soil Erosion Res. Lab., West Lafayette, Indiana, 1989.

Garde, R. J., and K. G. R. Raju, *Mechanics of Sediment Transportation and Alluvial Stream Problems*, 2nd ed., 618 pp., John Wiley, New York, 1985.

Govers, G., Evaluation of transporting capacity formulae for overland flow, in *Overland Flow Hydraulics and Erosion Mechanics*, edited by A. J. Parsons and A. D. Abrahams, pp. 243–273, Chapman and Hall, New York, 1992.

Gray, D. H., and W. F. Megahan, Forest vegetation removal and slope stability in the Idaho batholith, *USDA For. Serv. Res. Pap. INT-271*, 23 pp., For. and Range Exp. Stn., Ogden, Utah, 1981.

Gupta, H. V., S. Sorooshian, and P. O. Yapo, Toward improved calibration of hydrologic models: Multiple and noncommensurable measures of information, *Water Resour. Res.*, *34*(4), 751–763, 1998.

Hancock, G., and G. Willgoose, Use of a landscape simulator in the validation of the SIBERIA catchment evolution model: Declining equilibrium landforms, *Water Resour. Res.*, *37*(7), 1981–1992, 2001.

Hancock, G. R., G. R. Willgoose, and K. G. Evans, Testing the Siberia landscape evolution model using the Tin Camp Creek, northern territory, Australia, field catchment, *Earth Surf. Processes Landforms*, *27*(2), 125–143, 2001.

Hashimoto, H., A comparison between gravity flows of dry sand and sand-water mixtures, in *Recent Developments in Debris Flows*, edited by A. Armanini and M. Michiue, pp. 70–92, Springer-Verlag, New York, 1997.

Istanbulluoglu, E., D. G. Tarboton, R. T. Pack, and C. Luce, A probabilistic approach for channel initiation, *Water Resour. Res.*, *38*(12), 1325, doi:10.1029/2001WR000782, 2002.

Jan, C. D., and H. W. Shen, Review dynamic modeling of debris flows, in *Recent Developments in Debris Flows*, edited by A. Armanini and M. Michiue, pp. 93–116, Springer-Verlag, New York, 1997.

Julien, P. Y., and D. B. Simons, Sediment transport capacity of overland flow, *Trans. ASAE*, *28*(3), 755–762, 1985.

Kirchner, J. W., R. C. Finkel, C. S. Riebe, D. E. Granger, J. L. Clayton, J. G. King, and W. F. Megahan, Mountain erosion over 10 yr, 10 k.y., and 10 m.y. time scales, *Geology*, *29*(7), 591–594, 2001.

Kirkby, M. J., Hillslope process-response models based on the continuity equation, in *Slopes Form and Processes*, *Spec. Publ. 3.*, pp. 15–30, Inst. of Br. Geogr., London, 1971.

Knighton, D., *Fluvial Forms and Processes*, 383 pp., Arnold, London, 1998.

Lane, L. J., and M. A. Nearing (Eds.), *USDA-Water Erosion Prediction Project: Hillslope Profile Model Documentation*, *NSERL Rep. 2*, Natl. Soil Erosion Res. Lab., West Lafayette, Indiana, 1989.

Laursen, E. M., The total sediment load of streams, *J. Hydraul. Div. Am. Soc. Civ. Eng.*, *84*(1530), 1–6, 1958.

Leopold, L. B., M. G. Wolman, and J. P. Miller, *Fluvial Processes in Geomorphology*, 522 pp., W. H. Freeman, New York, 1964.

Megahan, W. F., Erosion over time on severely disturbed granitic soils: A model, *USDA For. Serv. Res. Pap.*, *INT-156*, 14 pp., Intermountain For. and Range Exp. Stn., Ogden, Utah, 1974.

Megahan, W. F., An overview of erosion and sedimentation processes on granitic soils, in *Proceedings of the Decomposed Granite Soils Conference*, pp. 11–30, Davis, Calif., 1992.

Megahan, W. F., and W. J. Kidd, Effect of logging roads on sediment production rates in the Idaho batholith, *USDA For. Serv. Res. Pap.*, *INT-123*, 14 pp., For. Serv., Intermountain Res. Stn., Ogden, Utah, 1972.

Meyer, G. A., and S. G. Wells, Fire-related sedimentation events on alluvial fans, Yellowstone National Park, U.S.A., *J. Sediment. Res., Sect. A*, *67*, 776–791, 1997.

Meyer, G. A., J. L. Pierce, S. H. Wood, and A. J. T. Jull, Fire, storms and erosional events in the Idaho batholith, *Hydrol. Processes*, *15*, 3025–3038, 2001.

Meyer-Peter, E., and R. Muller, Formulas for bedload transport, paper presented at the Third Conference of the International Association of Hydraulic Research, Stockholm, Sweden, 1948.

Mizuyama, T., Bedload transport in steep channels, Ph.D. thesis, Kyoto Univ., Kyoto, Japan, 1977.

Mizuyama, T., and H. Shimohigashi, Influence of fine sediment concentration on sediment transport rates (in Japanese), *Jpn. Civ. Eng. J.*, *27*(1), 46–49, 1985.

Montgomery, D. R., Road surface drainage, channel initiation, and slope instability, *Water Resour. Res.*, *30*(6), 1925–1932, 1994.

Moore, I. D., and G. J. Burch, Sediment transport capacity of sheet and rill flow: Application of unit stream power theory, *Water Resour. Res.*, *22*(8), 1350–1360, 1986.

Nearing, M. A., L. D. Norton, D. A. Bulgakov, G. A. Larinov, L. T. West, and K. M. Dontsova, Hydraulics and erosion in eroding rills, *Water Resour. Res.*, *33*(4), 865–876, 1997.

Niemann, J. D., N. M. Gasparini, G. E. Tucker, and R. L. Bras, A quantitative evaluation of Playfair's law and its use in testing long-term stream erosion models, *Earth Surf. Processes Landforms*, *26*, 1317–1332, 2001.

Prosser, I. P., and C. J. Slade, Gully formation and the role of valley floor vegetation, southeastern Australia, *Geology*, *22*, 1127–1130, 1994.

Prosser, I. P., and M. Soufi, Controls on gully formation following forest clearing in a humid temperature environment, *Water Resour. Res.*, *34*(12), 3661–3671, 1998.

Rickenmann, D., Bedload transport and hyperconcentrated flow at steep slopes, in *Fluvial Hydraulics of Mountain Regions*, edited by A. Armanini and G. D. Silvio, pp. 429–441, Springer-Verlag, New York, 1991.

Rickenmann, D., Hyperconcentrated flow and sediment transport at steep slopes, *J. Hydraul. Eng.*, *117*(11), 1419–1439, 1992.

Rickenmann, D., Emperical relationships for debris flows, *Nat. Hazards*, *19*, 47–77, 1999.

Rodriguez-Iturbe, I., and A. Rinaldo, *Fractal River Basins*, 547 pp., Cambridge Univ. Press, New York, 1997.

Schumm, S. A., M. D. Harvey, and C. C. Watson, *Incised Channels: Morphology Dynamics and Control*, 200 pp., Water Resour. Publ., Highlands Ranch, Colo., 1984.

Selby, M. J., *Hillslope Materials and Processes*, 451 pp., Oxford Univ. Press, New York, 1993.

Sidorchuk, A., Dynamic and static models of gully erosion, *Catena*, *37*, 401–414, 1999.

Simons, D. B., and F. Senturk, *Sediment Transport Technology*, 807 pp., Water Resour. Publ., Highlands Ranch, Colo., 1977.

Smart, G., Sediment transport formula for steep channels, *J. Hydraul. Eng.*, *100*(3), 267–276, 1984.

Smart, G. M., and M. Jaeggi, Sediment transport on steep slopes, Mitt. der Versuchsanst. fur Wasserbau, Hydrol. und Glaziol., *64*, Zurich Inst. of Technol., Zurich, Switzerland, 1983.

Smith, T. R., and F. P. Bretherton, Stability and the conservation of mass in drainage basin evolution, *Water Resour. Res.*, *8*(6), 1506–1529, 1972.

Suszka, L., Modification of transport rate formula for steep channels, in *Fluvial Hydraulics of Mountain Regions*, edited by A. Armanini and G. G. Silvio, pp. 59–70, Springer-Verlag, New York, 1991.

Tarboton, D. G., A new method for the determination of flow directions and contributing areas in grid digital elevation models, *Water Resour. Res.*, *33*(2), 309–319, 1997.

Tarboton, D. G., R. L. Bras, and I. Rodriguez-Iturbe, On the extraction of channel networks from digital elevation data, *Hydrol. Processes*, *5*(1), 81–100, 1991.

Tarboton, D. G., R. L. Bras, and I. Rodriguez-Iturbe, A physical basis for drainage density, *Geomorphology*, *5*(1/2), 59–76, 1992.

Tucker, G. E., and R. L. Bras, Hillslope processes, drainage density and landscape morphology, *Water Resour. Res.*, *34*(10), 2751–2764, 1998.

Tucker, G. E., and K. X. Whipple, Topographic outcomes predicted by stream erosion models: Sensitivity analysis and intermodel comparison, *J. Geophys. Res.*, *107*(B9), 2179, doi:10.1029/2001JB000162, 2002.

Vandekerckhove, L., J. Poesen, D. O. Wijdenes, and T. D. Figueiredo, Topographic thresholds for ephemeral gully initiation in intensely cultivated areas of the Mediterranean, *Catena*, *33*, 271–292, 1998.

Vandekerckhove, L., J. Poesen, D. O. Wijdenes, J. Nachtergaele, C. Kosmas, M. J. Roxo, and T. D. Figueiredo, Thresholds for gully initiation and sedimentation in Mediterranean Europe, *Earth Surf. Processes Landforms*, *25*, 1201–1220, 2000.

Wemple, B. C., J. A. Jones, and G. E. Grant, Channel network extension by logging roads in two basins, western Cascades, Oregon, *Water Resour. Bull.*, *32*(6), 1195–1207, 1996.

Whipple, K. X., and G. E. Tucker, Dynamics of the stream-power river incision model: Implications for height limits of mountain ranges, land-

scape response timescales, and research needs, *J. Geophys. Res.*, *104*(B8), 17,661–17,674, 1999.

Willgoose, G. R., A physically based channel network and catchment evolution model, Ph.D. thesis, Mass. Inst. of Technol., Cambridge, Mass., 1989.

Willgoose, G. R., A physical explanation of an observed area-slope relationship for catchments with declining relief, *Water Resour. Res.*, *30*, 151–159, 1994.

Willgoose, G., R. L. Bras, and I. Rodriguez-Iturbe, A coupled channel network growth and hillslope evolution model: 1. Theory, *Water Resour. Res.*, *27*(7), 1671–1684, 1991a.

Willgoose, G., R. L. Bras, and I. Rodriguez-Iturbe, A physical explanation of an observed link area-slope relationship, *Water Resour. Res.*, *27*(7), 1697–1702, 1991b.

Woodward, D. E., Method to predict cropland ephemeral gully erosion, *Catena*, *37*, 393–399, 1999.

Woolhiser, D. A., R. E. Smith, and D. C. Goodrich, KINEROS, A kinematic runoff and erosion model: Documentation and user manual, *Rep. ARS-77*, Agric. Res. Serv., U. S. Dep. of Agric., Tuscon, Ariz., 1990.

Yalin, M. S., *Mechanics of Sediment Transport*, 2nd ed., Pergamon, New York, 1977.

E. Istanbulluoglu, Department of Civil and Environmental Engineering, Massachusetts Institute of Technology, 77 Massachusetts Avenue, Room 48-114, Cambridge, MA 02139, USA. (erkan@mit.edu)

C. Luce, Rocky Mountain Research Station, U.S. Forest Service, Boise, ID 83702, USA. (cluce@fs.fed.edu)

R. T. Pack and D. G. Tarboton, Civil and Environmental Engineering Department, Utah State University, 4110 Old Main Hill, Logan, UT 84322-4110, USA. (dtarb@cc.usu.edu)